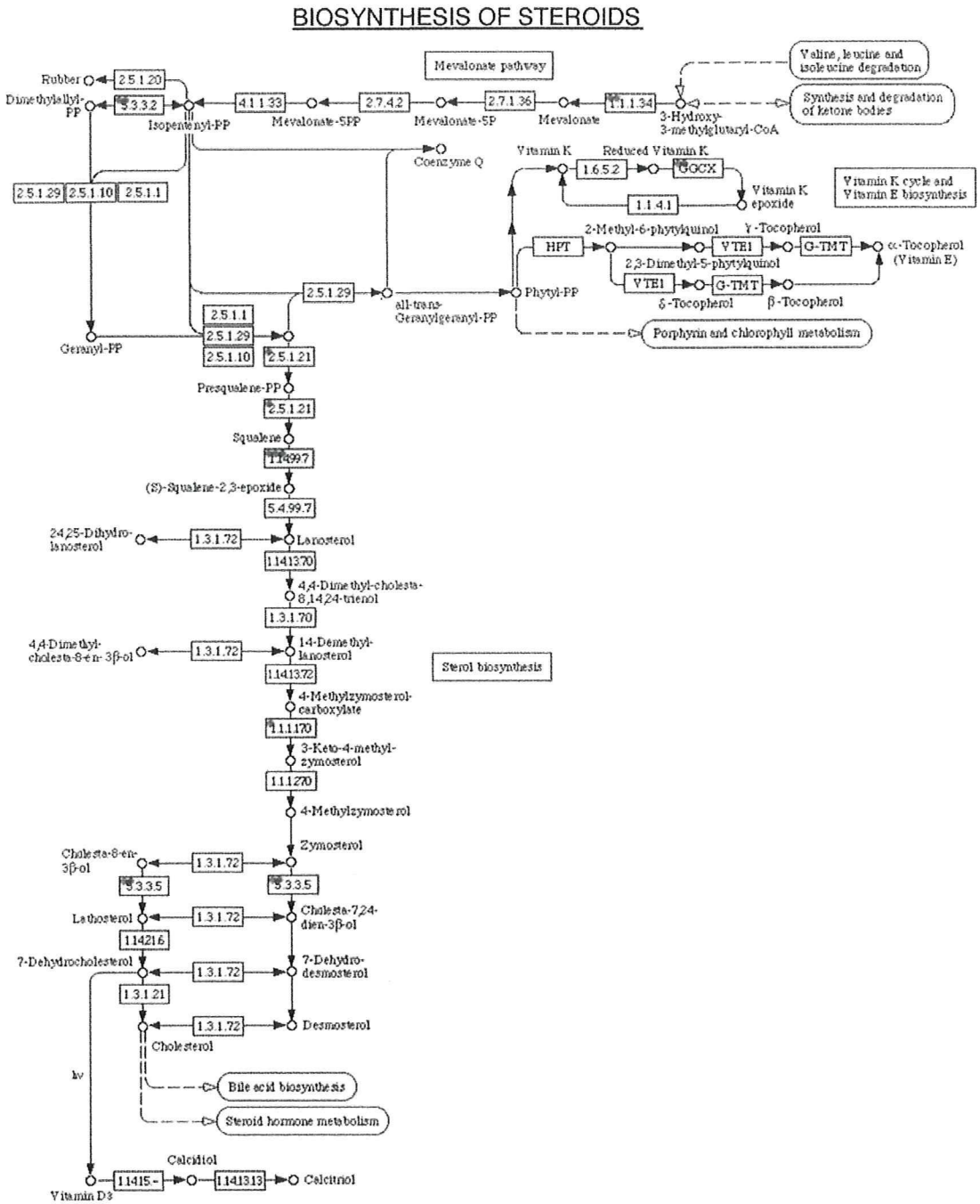

Fig. 5 KEGG Pathway map and array data (biosynthesis of steroids). Gene expression changes were mapped on the pathways. Each *circle* within a *box* represents the corresponding probe set on Human Genome U133 Plus 2.0 array because multiple probe sets are sometimes designed for a single gene. *Red circles* indicate overexpressed genes in *cured* cells compared to parental Huh7 cells. The *dotted numerical code* in each *box* represents the Enzyme Commission (EC) number based on the recommendations of the Nomenclature Committee of the International Union of Biochemistry and Molecular Biology (IUBMB). Correspondence between the genes that were examined in the microarray analyses and enzymes that are presented in Fig. 5 is shown in Supplementary Table 4

Rep-Feo cells showed that the replication of the HCV replicon was suppressed by clofibrate and fenofibrate in a dose-dependent manner, whereas pioglitazone and troglitazone elevated expression levels of replicon. The MTS assay did not show any effect on cell viability or replication. These results suggest that the decrease or increase in HCV replication is due to specific effects of PPAR-alpha or gamma agonists on HCV replication.

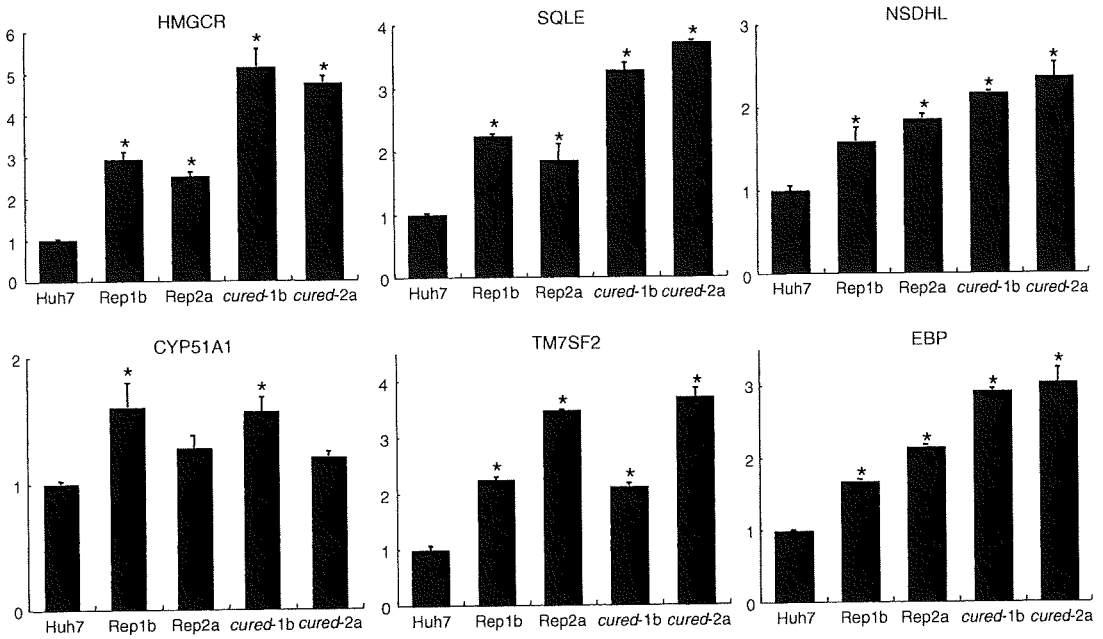

Fig. 6 Real-time detection RT-PCR. Real-time RT-PCR was performed to verify expression levels of genes that were listed in the cholesterol biosynthesis pathway in Fig. 4c and that showed differences in their expression levels by microarray analyses. Assays were done in triplicate, and *asterisks* indicate *P*-values of less than 0.05

Discussion

In our present analyses, we identified MAPK signaling, biosynthesis of steroid related and TGF-beta signaling pathways as significantly changed pathway processes by comparing replicon-expressing and *cured* cells (Supplementary Table 2). The results suggest that these pathways were primarily affected by HCV replication. Comparison of *cured* cells and naïve Huh7 cells identified cell cycle, TGF-beta, sphingolipid metabolism, and biosynthesis of steroids pathways as significantly changed pathways. Interestingly, cholesterol biosynthesis pathways were significantly changed in both comparisons (Supplementary Tables 2, 3). These data suggest that these pathways may positively regulate cellular HCV replication and that cholesterol biosynthesis pathways are primarily activated by HCV replication and may be essential for continuous virus replication.

There are several studies that report gene expression changes in replicon-expressing Huh7 cells as compared with the naïve cells [30–32]. In those studies, however, the changes in gene expression do not only reflect the effect of intracellular HCV replication, but also reflect alteration of host cell clonalities. Indeed, there are inconsistencies among studies. Use of the cured Huh7 cells can minimize the effect of cellular clonal changes because such Huh7 subclones have already been selected through HCV replicon transduction, drug-resistance selection and subsequent HCV elimination [33]. In our study, we have compared gene expression between genotype 1b and 2a replicon cells, respective cured cells and the naïve parental cells, and have identified molecular signaling or metabolic pathways that were differentially up- or down-regulated over different HCV genotypes.

Comprehensive microarray analyses and pathway analyses were very useful for the identification of molecular mechanisms of HCV infection and replication in the host cells. We used the KEGG Pathway database [28], a knowledge-based database of biological systems that integrates genomic, chemical and systemic functional information. KEGG provides a reference knowledge base for linking genome to life through the process of PATHWAY mapping, which is to map, for example, a genomic or transcriptomic content of genes to KEGG reference pathways to infer systemic behavior of the cells or the organism. These pathway databases are free on-line resources. Using these analyses, the close relation between cholesterol metabolism and HCV replication was demonstrated. Moreover, in relation to this, when we examined the pathways of other lipid metabolism, it was shown that fatty acid biosynthesis metabolism-related pathways were significantly changed in *cured* cells, and indeed we found a large number of lipid droplets in the cytosol of replicon cells and *cured* cells.

The HCV-JFH1 strain is the basis of a robustly replicating cell culture system reported recently [5]. We have performed comprehensive gene expression analyses using the HCV-JFH1 and the cured Huh7.5.1 cell line [6]. The

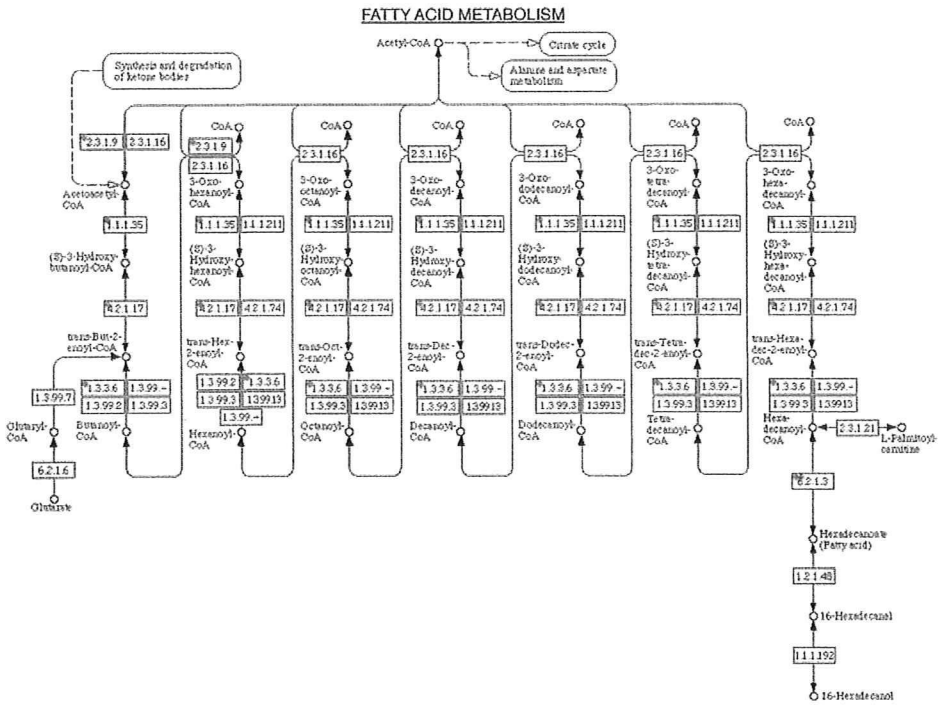

Fig. 7 KEGG Pathway map and array data (fatty acid metabolism). Gene expression changes were mapped on the pathways. Each *circle* within a *box* represents the corresponding probe set on Human Genome U133 Plus 2.0 array because multiple probe sets are sometimes designed for a single gene. *Red circles* indicate overexpressed genes in *cured* cells compared to parental Huh7 cells. The *dotted numerical code* in each *box* represents the Enzyme Commission (EC) number. Correspondence between the genes that were examined in the microarray analyses and enzymes that are presented in Fig. 7 are shown in Supplementary Table 4

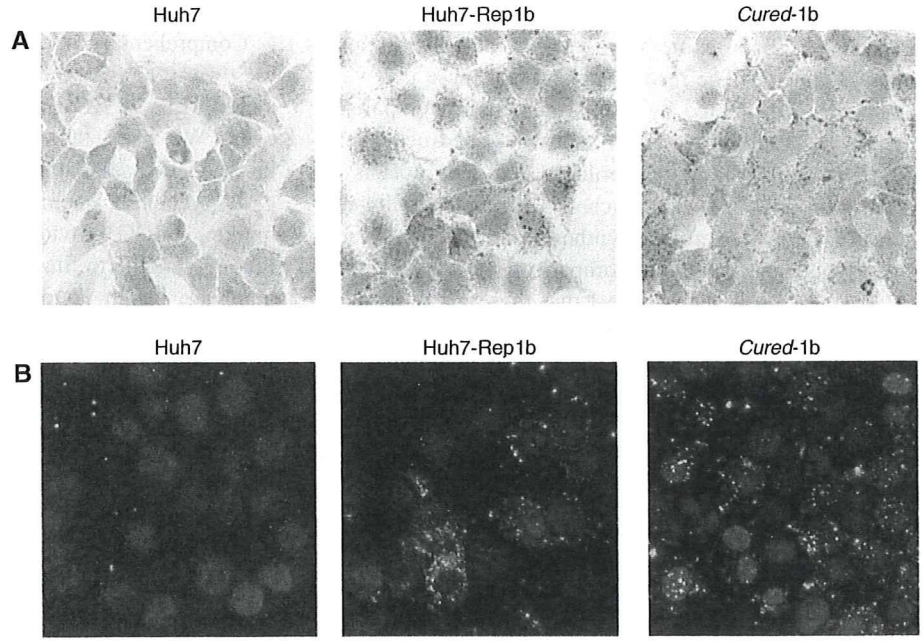

Fig. 8 Detection of intracellular lipid droplets and HCV NS protein. **a** Huh7 cells, replicon cells and *cured* cells were fixed and stained with Oil red O and Mayer's hematoxylin. Intracellular lipid droplets were detected as *red spheres* in the cells. Nuclei are stained in *blue*. **b** Rep1b/Huh7 cells were labeled with antibodies against NS5A (*red*). Lipid droplets and nuclei were stained with BODIPY493/503 (*green*) and DAPI (*blue*), respectively

KEGG Pathway analyses have identified several significantly affected pathways that are involved in the cell cycle, TGF-beta signaling, PPAR signaling and sterol biosynthesis. These findings are consistent with our present results using the HCV subgenomic replicon (see the Supplementary Table 5; Supplementary Figs. 4, 5).

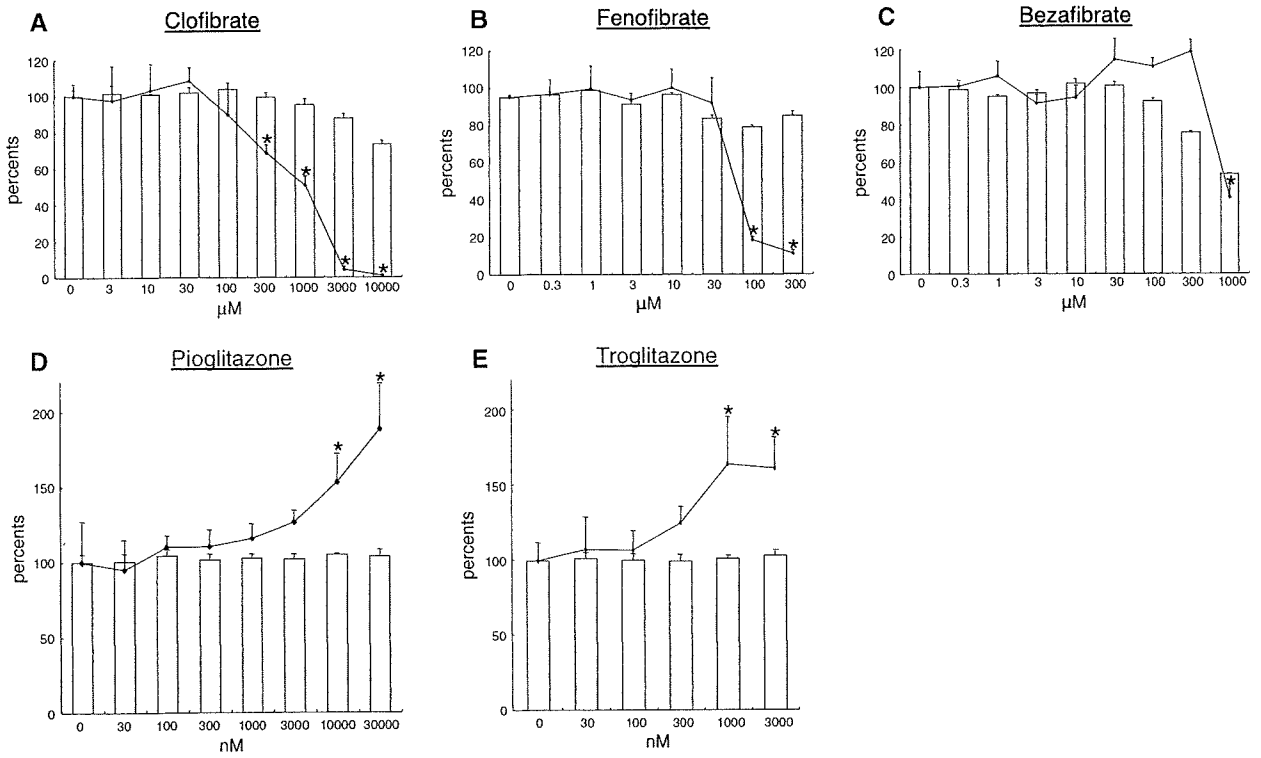

Fig. 9 Results of secondary screening with PPAR-alpha and -gamma agonists. Luciferase activity for HCV replication levels is shown as a percentage of the control. Cell viability is also shown as percentage of the control. Each *bar* represents the average of quadruplicate data points with standard deviation represented as the *error bar*. *Asterisks* denotes a significant difference from the control of at least $P < 0.05$

The JFH1 strain, however, showed substantial cytopathic effects on cultures of more than 5 days accompanied by overall induction of apoptosis-related genes and massive cell death [34]. Thus, it was difficult to conduct gene expression studies consistently.

Lipid metabolism is involved in the life cycle of many viruses. Recent studies have demonstrated the localization of HCV nonstructural proteins in the lipid raft in the endoplasmic reticulum (ER) forming intracellular replication complexes, called membranous webs [35, 36]. Because the lipid raft is enriched in cholesterols and sphingolipids, depletion of these lipids leads to inhibition of HCV genomic replication [19]. Amemiya et al. [37] reported that another serine palmitoyltransferase, myriocin, depleted cellular sphingomyelin contents and inhibited HCV replication.

It has been reported that statins efficiently suppress HCV replication in vitro and in vivo [38–40]. Statins are inhibitors of HMG-CoA reductase and shut down cholesterol biosynthesis by preventing the formation of mevalonate from 3-hydroxy-3-methyl-glutaryl CoA. As we have shown in the results, all enzymes in the cholesterol synthesis pathway were upregulated in the replicon-expressing and the cured Huh7 cells. In addition to lowering intracellular levels of sterols, statins also reduce levels of isoprenoids, which are derived from mevalonate. Isoprenoids such as farnesyl pyrophosphate and geranylgeranyl pyrophosphate serve as lipid attachments for a variety of intracellular signaling molecules. In our results, the cholesterol biosynthesis pathway was also upregulated between cured versus naïve cell lines as well as replicon versus cured cell lines. These results suggest that HCV replication may promote synthesis of lipids including steroids that were essential for the viral efficient replication.

It has been recognized that HCV infection causes hepatic steatosis and subclinical insulin resistance and that they are independent of other risk factors such as obesity or the presence of diabetes mellitus. Similarly, in HCV cell cultures, Yang et al. [41] have reported that cellular fatty acid synthase is upregulated in HCV-infected Huh7 cells and specific inhibition of the enzymatic activity caused suppression of HCV replication. In the present study, although lipid metabolism-related genes were upregulated in cured cells, which supports efficient HCV replication, there was not significant change in lipid-related genes between replicon-expressing as compared with cured cells (Fig. 7). These results suggest that HCV subgenomic replication does not cause steatosis as it did in full-length HCV cell culture [41]. These discrepancies might be due to the absence of the presence of HCV structural genes including core and envelope proteins.

We have shown an increase in lipid droplets in HCV replicon-positive cells and their cured cell lines as a phenotype of the gene expression profiles (Fig. 8). On the other hand, ACOX1, a rate-limiting enzyme of peroxisomal beta-oxidation, was higher in cured cells than parental Huh7 cells (Fig. 7) [42]. We have shown preliminarily that cellular SREBP1 (sterol regulatory element-binding protein 1), which regulates a set of triglyceride synthesis enzymes en bloc, is upregulated in HCV replicon-positive cell lines. These discrepancies might be due to more proficient activation of SREBP1-induced fatty acid biosynthesis pathways. Collectively, our results suggest that the overall fatty acid synthesis pathway, not only fatty acid synthase, is activated by upregulation of a set of responsible enzymes.

We have investigated effects of PPAR agonists to HCV replication. PPAR-alpha agonists, clofibrate and fenofibrate suppressed HCV replication (Fig. 9). PPAR-alpha, not PPAR-gamma, is expressed in hepatocytes, recognizes cellular free fatty acids and leukotriene B4 as a specific ligands, and mediates oxidative degradation of triglyceride and depletion of intracellular fat droplets [43, 44]. These properties of PPAR-alpha agonists suggest that the level of HCV replication is affected by the increased production of fatty acids, but not by the overexpression of their related enzymes. PPAR-gamma agonists, in contrast, amplified HCV replication. Because PPAR-gamma is a regulator of fatty acid metabolism in peripheral tissue and is not expressed in the hepatocytes or in Huh7 cells (data not shown), it is possible that the effects of the PPAR-gamma agonists on HCV replication may be through its pleiotropic side effects such as p38 MAPK activation [45]. Very recently, it has been reported that HCV-NS5A proteins induce expression of PPARgamma [46].

In conclusion, comprehensive gene expression and pathway analyses were useful to study molecular pathways that were involved in HCV pathogeneses and to identify host factors for HCV replication that could constitute antiviral targets.

Acknowledgment This study was supported by grants from Ministry of Education, Culture, Sports, Science and Technology-Japan, the Japan Society for the Promotion of Science, Ministry of Health, Labour and Welfare-Japan, Japan Health Sciences Foundation, and National Institute of Biomedical Innovation.

References

1. Alter MJ. Epidemiology of hepatitis C. Hepatology. 1997;26:62S–5S.
2. Hadziyannis SJ, Sette H Jr, Morgan TR, Balan V, Diago M, Marcellin P, et al. Peginterferon-alpha2a and ribavirin combination therapy in chronic hepatitis C: a randomized study of treatment duration and ribavirin dose. Ann Intern Med. 2004;140:346–55.
3. Sakamoto N, Watanabe M. New therapeutic approaches to hepatitis C virus. J Gastroenterol. 2009;44:643–9.
4. Lohmann V, Korner F, Koch J, Herian U, Theilmann L, Bartenschlager R. Replication of subgenomic hepatitis C virus RNAs in a hepatoma cell line. Science. 1999;285:110–3.
5. Wakita T, Pietschmann T, Kato T, Date T, Miyamoto M, Zhao Z, et al. Production of infectious hepatitis C virus in tissue culture from a cloned viral genome. Nat Med. 2005;11:791–6.
6. Zhong J, Gastaminza P, Cheng G, Kapadia S, Kato T, Burton DR, et al. Robust hepatitis C virus infection in vitro. Proc Natl Acad Sci USA. 2005;102:9294–9.
7. Tai AW, Benita Y, Peng LF, Kim SS, Sakamoto N, Xavier RJ, et al. A functional genomic screen identifies cellular cofactors of hepatitis C virus replication. Cell Host Microbe. 2009;5:298–307.
8. Itsui Y, Sakamoto N, Kurosaki M, Kanazawa N, Tanabe Y, Koyama T, et al. Expressional screening of interferon-stimulated genes for antiviral activity against hepatitis C virus replication. J Viral Hepat. 2006;13:690–700.
9. Yamashiro T, Sakamoto N, Kurosaki M, Kanazawa N, Tanabe Y, Nakagawa M, et al. Negative regulation of intracellular hepatitis C virus replication by interferon regulatory factor 3. J Gastroenterol. 2006;41:750–7.
10. Foy E, Li K, Sumpter R Jr, Loo YM, Johnson CL, Wang C, et al. Control of antiviral defenses through hepatitis C virus disruption of retinoic acid-inducible gene-I signaling. Proc Natl Acad Sci USA. 2005;102:2986–91.
11. Sakamoto N, Yoshimura M, Kimura T, Toyama K, Sekine-Osajima Y, Watanabe M, et al. Bone morphogenetic protein-7 and interferon-alpha synergistically suppress hepatitis C virus replicon. Biochem Biophys Res Commun. 2007;357:467–73.
12. Murata T, Ohshima T, Yamaji M, Hosaka M, Miyanari Y, Hijikata M, et al. Suppression of hepatitis C virus replicon by TGF-beta. Virology. 2005;331:407–17.
13. Shimakami T, Honda M, Kusakawa T, Murata T, Shimotohno K, Kaneko S, et al. Effect of hepatitis C virus (HCV) NS5B-nucleolin interaction on HCV replication with HCV subgenomic replicon. J Virol. 2006;80:3332–40.
14. Nakagawa M, Sakamoto N, Tanabe Y, Koyama T, Itsui Y, Takeda Y, et al. Suppression of hepatitis C virus replication by cyclosporin a is mediated by blockade of cyclophilins. Gastroenterology. 2005;129:1031–41.
15. Tardif KD, Mori K, Siddiqui A. Hepatitis C virus subgenomic replicons induce endoplasmic reticulum stress activating an intracellular signaling pathway. J Virol. 2002;76:7453–9.
16. Wang J, Tong W, Zhang X, Chen L, Yi Z, Pan T, et al. Hepatitis C virus non-structural protein NS5A interacts with FKBP38 and inhibits apoptosis in Huh7 hepatoma cells. FEBS Lett. 2006;580:4392–400.
17. Choi YW, Tan YJ, Lim SG, Hong W, Goh PY. Proteomic approach identifies HSP27 as an interacting partner of the hepatitis C virus NS5A protein. Biochem Biophys Res Commun. 2004;318:514–9.
18. Okamoto T, Nishimura Y, Ichimura T, Suzuki K, Miyamura T, Suzuki T, et al. Hepatitis C virus RNA replication is regulated by FKBP8 and Hsp90. EMBO J. 2006;25:5015–25.
19. Sakamoto H, Okamoto K, Aoki M, Kato H, Katsume A, Ohta A, et al. Host sphingolipid biosynthesis as a target for hepatitis C virus therapy. Nat Chem Biol. 2005;1:333–7.
20. Yokota T, Sakamoto N, Enomoto N, Tanabe Y, Miyagishi M, Maekawa S, et al. Inhibition of intracellular hepatitis C virus replication by synthetic and vector-derived small interfering RNAs. EMBO Rep. 2003;4:602–8.
21. Tanabe Y, Sakamoto N, Enomoto N, Kurosaki M, Ueda E, Maekawa S, et al. Synergistic inhibition of intracellular hepatitis C virus replication by combination of ribavirin and interferon-alpha. J Infect Dis. 2004;189:1129–39.

22. Guo JT, Bichko VV, Seeger C. Effect of alpha interferon on the hepatitis C virus replicon. J Virol. 2001;75:8516–23.
23. Donnelly MLL, Hughes LE, Luke G, Mendoza H, ten Dam E, Gani D, et al. The 'cleavage' activities of foot-and-mouth disease virus 2A site-directed mutants and naturally occurring '2A-like' sequences. J Gen Virol. 2001;82:1027–41.
24. Nakagawa M, Sakamoto N, Enomoto N, Tanabe Y, Kanazawa N, Koyama T, et al. Specific inhibition of hepatitis C virus replication by cyclosporin A. Biochem Biophys Res Commun. 2004;313:42–7.
25. Blight KJ, McKeating JA, Rice CM. Highly permissive cell lines for subgenomic and genomic hepatitis C virus RNA replication. J Virol. 2002;76:13001–14.
26. Strand C, Enell J, Hedenfalk I, Ferno M. RNA quality in frozen breast cancer samples and the influence on gene expression analysis—a comparison of three evaluation methods using microcapillary electrophoresis traces. BMC Mol Biol. 2007;8:38.
27. Tusher VG, Tibshirani R, Chu G. Significance analysis of microarrays applied to the ionizing radiation response. Proc Natl Acad Sci USA. 2001;98:5116–21.
28. Kanehisa M, Araki M, Goto S, Hattori M, Hirakawa M, Itoh M, et al. KEGG for linking genomes to life and the environment. Nucleic Acids Res. 2008;36:D480–4.
29. Benjamini Y, Hochberg Y. Controlling the false discovery rate: a practical and powerful approach to multiple testing. J R Stat Soc B. 1995;57:289–300.
30. Ciccaglione AR, Marcantonio C, Tritarelli E, Tataseo P, Ferraris A, Bruni R, et al. Microarray analysis identifies a common set of cellular genes modulated by different HCV replicon clones. BMC Genomics. 2008;9:309.
31. Hayashi J, Stoyanova R, Seeger C. The transcriptome of HCV replicon expressing cell lines in the presence of alpha interferon. Virology. 2005;335:264–75.
32. Scholle F, Li K, Bodola F, Ikeda M, Luxon BA, Lemon SM. Virus–host cell interactions during hepatitis C virus RNA replication: impact of polyprotein expression on the cellular transcriptome and cell cycle association with viral RNA synthesis. J Virol. 2004;78:1513–24.
33. Abe K, Ikeda M, Dansako H, Naka K, Shimotohno K, Kato N. cDNA microarray analysis to compare HCV subgenomic replicon cells with their cured cells. Virus Res. 2005;107:73–81.
34. Sekine-Osajima Y, Sakamoto N, Nakagawa M, Itsui Y, Tasaka M, Nishimura-Sakurai Y, et al. Development of plaque assays for hepatitis C virus and isolation of mutants with enhanced cytopathogenicity and replication capacity. Virology. 2008;371:71–85.
35. Mottola G, Cardinali G, Ceccacci A, Trozzi C, Bartholomew L, Torrisi MR, et al. Hepatitis C virus nonstructural proteins are localized in a modified endoplasmic reticulum of cells expressing viral subgenomic replicons. Virology. 2002;293:31–43.
36. Gosert R, Egger D, Lohmann V, Bartenschlager R, Blum HE, Bienz K, et al. Identification of the hepatitis C virus RNA replication complex in Huh-7 cells harboring subgenomic replicons. J Virol. 2003;77:5487–92.
37. Amemiya F, Maekawa S, Itakura Y, Kanayama A, Takano S, Yamaguchi T, et al. Targeting lipid metabolism in the treatment of hepatitis C. J Infect Dis. 2008;197:361–70.
38. Ikeda M, Abe K, Yamada M, Dansako H, Naka K, Kato N. Different anti-HCV profiles of statins and their potential for combination therapy with interferon. Hepatology. 2006;44:117–25.
39. Kim SS, Peng LF, Lin W, Choe WH, Sakamoto N, Kato N, et al. A cell-based, high-throughput screen for small molecule regulators of hepatitis C virus replication. Gastroenterology. 2007;132:311–20.
40. Bader T, Fazili J, Madhoun M, Aston C, Hughes D, Rizvi S, et al. Fluvastatin inhibits hepatitis C replication in humans. Am J Gastroenterol. 2008;103:1383–9.
41. Yang W, Hood BL, Chadwick SL, Liu S, Watkins SC, Luo G, et al. Fatty acid synthase is up-regulated during hepatitis C virus infection and regulates hepatitis C virus entry and production. Hepatology. 2008;48:1396–403.
42. Li Y, Tharappel JC, Gooper S, Glenn M, Glauert HP, Spear BT. Expression of the hydrogen peroxide-generating enzyme fatty acyl CoA oxidase activates NF-kappaB. DNA Cell Biol. 2000;19:113–20.
43. Costet P, Legendre C, More J, Edgar A, Galtier P, Pineau T. Peroxisome proliferator-activated receptor alpha-isoform deficiency leads to progressive dyslipidemia with sexually dimorphic obesity and steatosis. J Biol Chem. 1998;273:29577–85.
44. Kersten S, Seydoux J, Peters JM, Gonzalez FJ, Desvergne B, Wahli W. Peroxisome proliferator-activated receptor alpha mediates the adaptive response to fasting. J Clin Invest. 1999;103:1489–98.
45. Schiefelbein D, Seitz O, Goren I, Dissmann JP, Schmidt H, Bachmann M, et al. Keratinocyte-derived vascular endothelial growth factor biosynthesis represents a pleiotropic side effect of peroxisome proliferator-activated receptor-gamma agonist troglitazone but not rosiglitazone and involves activation of p38 mitogen-activated protein kinase: implications for diabetes-impaired skin repair. Mol Pharmacol. 2008;74:952–63.
46. Kim K, Kim KH, Ha E, Park JY, Sakamoto N, Cheong J. Hepatitis C virus NS5A protein increases hepatic lipid accumulation via induction of activation and expression of PPARgamma. FEBS Lett. 2009;583:2720–6.
47. Kato T, Date T, Miyamoto M, Furusaka A, Tokushige K, Mizokami M, et al. Efficient replication of the genotype 2a hepatitis C virus subgenomic replicon. Gastroenterology. 2003;125:1808–17.

J Gastroenterol
DOI 10.1007/s00535-009-0132-9

ORIGINAL ARTICLE—LIVER, PANCREAS, AND BILIARY TRACT

Inhibition of hepatitis C virus replication by chloroquine targeting virus-associated autophagy

Tomokazu Mizui · Shunhei Yamashina · Isei Tanida · Yoshiyuki Takei · Takashi Ueno · Naoya Sakamoto · Kenichi Ikejima · Tsuneo Kitamura · Nobuyuki Enomoto · Tatsuo Sakai · Eiki Kominami · Sumio Watanabe

Received: 28 May 2009 / Accepted: 22 August 2009
© Springer 2009

Abstract
Background Autophagy has been reported to play a pivotal role on the replication of various RNA viruses. In this study, we investigated the role of autophagy on hepatitis C virus (HCV) RNA replication and demonstrated anti-HCV effects of an autophagic proteolysis inhibitor, chloroquine.
Methods Induction of autophagy was evaluated following the transfection of HCV replicon to Huh-7 cells. Next, we investigated the replication of HCV subgenomic replicon in response to treatment with lysosomal protease inhibitors or pharmacological autophagy inhibitor. The effect on HCV replication was analyzed after transfection with siRNA of ATG5, ATG7 and light-chain (LC)-3 to replicon cells. The antiviral effect of chloroquine and/or interferon-α (IFNα) was evaluated.
Results The transfection of HCV replicon increased the number of autophagosomes to about twofold over untransfected cells. Pharmacological inhibition of autophagic proteolysis significantly suppressed expression level of HCV replicon. Silencing of autophagy-related genes by siRNA transfection significantly blunted the replication of HCV replicon. Treatment of replicon cells with chloroquine

T. Mizui (✉) · S. Yamashina · K. Ikejima · T. Kitamura · S. Watanabe
Department of Gastroenterology, Juntendo University, School of Medicine, Hongo 2-1-1, Bunkyo-ku, Tokyo 113-8421, Japan
e-mail: don-chip@aqua.email.ne.jp

S. Yamashina
e-mail: ryou0607jp@ybb.ne.jp

K. Ikejima
e-mail: ikejima@juntendo.ac.jp

T. Kitamura
e-mail: kitamura@juntendo.ac.jp

S. Watanabe
e-mail: sumio@juntendo.ac.jp

I. Tanida
Department of Biochemistry and Cell Biology, Laboratory of Biomembranes, National Institute of Infectious Disease, Toyama 1-23-1, Shinjuku-ku, Tokyo 162-8640, Japan
e-mail: tanida@nih.go.jp

Y. Takei
Department of Gastroenterology, Mie University, Kurimamachiya-cho 1577, Tsu, Mie 514-8507, Japan
e-mail: ytakei@clin.medic.mie-u.ac.jp

T. Ueno · E. Kominami
Department of Biochemistry, Juntendo University School of Medicine, Hongo 2-1-1, Bunkyo-ku, Tokyo 113-8421, Japan
e-mail: upfield@juntendo.ac.jp

E. Kominami
e-mail: kominami@juntendo.ac.jp

N. Sakamoto
Department of Gastroenterology and Hepatology, Tokyo Medical and Dental University, Yushima 1-5-45, Bunkyo-ku, Tokyo 113-8510, Japan
e-mail: nsakamoto.gast@tmd.ac.jp

N. Enomoto
First Department of Internal Medicine, University of Yamanashi, Kakedo 4-3-11, Kofu-shi, Yamanashi 400-8511, Japan
e-mail: enomoto@yamanashi.ac.jp

T. Sakai
Department of Anatomy, Juntendo University School of Medicine, Hongo 2-1-1, Bunkyo-ku, Tokyo 113-8421, Japan
e-mail: tatsuo@juntendo.ac.jp

Published online: 17 September 2009

suppressed the replication of the HCV replicon in a dose-dependent manner. Furthermore, combination treatment of chloroquine to IFNα enhanced the antiviral effect of IFNα and prevented re-propagation of HCV replicon. Protein kinase R was activated in cells treated with IFNα but not with chloroquine. Incubation with chloroquine decreased degradation of long-lived protein leucine.

Conclusion The results of this study suggest that the replication of HCV replicon utilizes machinery involving cellular autophagic proteolysis. The therapy targeted to autophagic proteolysis by using chloroquine may provide a new therapeutic option against chronic hepatitis C.

Keywords Autophagy · Autophagosome · HCV replicon · Chloroquine

Introduction

The genome of HCV, a member of the family Flaviviridae, consists of a positive-sense single-stranded RNA. Peg-interferon/ribavirin combination therapy, which is the most effective therapy against HCV infection, is effective in around 50% for genotype 1 and 80% for genotypes 2 and 3 [1–3], however, many people cannot tolerate the serious side effects and are resistant to Peg-interferon/ribavirin combination therapy. Difficulties in eradicating HCV are attributable to the limited number of treatment options against HCV [4, 5]. Therefore, the search for novel therapeutic agents remains a strong aspiration.

Autophagy is an evolutionarily conserved cellular pathway in which the cytoplasm and organelles are engulfed within double-membraned vesicles, known as autophagosomes. While cellular autophagy is thought to be in preparation for the turnover and recycling of cellular constituents [6–8], this process has been proposed as a mechanism of virus replication complex formation in positive-stranded RNA viruses including poliovirus, equine arteritis virus and coronavirus [9–12]. In these viruses, the replication complexes consist of double membrane vesicles in the cytoplasm, suggestive of an autophagosome origin [9, 12]. Recently, it was reported that transfection of HCV replicon induced autophagy [11]. Additionally, Sir et al. [13] demonstrated that the suppression of autophagy inhibited the replication of HCV. These findings suggested that the autophagy plays a pivotal role in HCV replication.

Chloroquine, which is widely used for the treatment of malaria, is a well-established inhibitor of autophagic proteolysis which acts by inhibiting acidification of lysosomes and endosomes [14]. It has been reported that chloroquine exerts direct antiviral effects on several RNA viruses including coronaviruses, flaviviruses and human immunodeficiency virus (HIV) [8, 15–17]. Moreover, clinical studies have demonstrated the safety, tolerability, and efficacy of chloroquine in the antiviral treatment of HIV infection [18, 19]. Here, we have demonstrated that autophagic proteolysis plays a pivotal role on HCV replication, moreover, the inhibition of autophagic proteolytic pathways can constitute an effective new therapeutic target against HCV.

Materials and methods

Cell culture and treatment

Huh-7 cells were stably transfected with HCV replicon expressing chimeric protein of firefly luciferase and neomycin phosphotransferase [20, 21]. They were cultured in Dulbecco's modified essential medium (DMEM) (Sigma, St. Louis, MO) supplemented with 10% foetal bovine serum (FBS) at 37°C under 5% CO_2. To maintain cell lines carrying the HCV replicon, G418 (Wako, Osaka, Japan) was added to the medium at a final concentration 500 μg/ml.

Luciferase assay

Luciferase activities were quantified to evaluate the replication of HCV replicon by a luminometer (Lumat LB9507; Berthold, Germany) using a Bright-Glo Luciferase Assay System (Promega, Madison, WI). Assays were performed in triplicate, and the results were expressed as mean ± SD as percents of controls.

Cell viability assay

The viability of cells was assessed by WST-1 assay. Cells were cultured in 96-well plates at 5×10^3/well for 24 h, and then treated with 3-methyladenine [22] (10 mM), mixture of E64d (1 μg/ml) and pepstatin A [23] (1 μg/ml), and chloroquine (10^{-6}–10^{-3} M) for 18 h. Cell proliferation reagent WST-1 (Roche, Swiss) was added to each well, and the cells were incubated for another 1 h at 37°C. The absorbance was measured against a background control by microplates reader (SPECTRA max 340PC, Molecular Devices, Sunnyvale, CA) at 450 nm. The reference wavelength was 650 nm.

Inhibition of autophagy and replication of HCV replicon

Cells were treated with 3-methyladenine (10 mM) or mixture of E64d (1 μg/ml) and pepstatin A (1 μg/ml), chloroquine (10^{-7}–10^{-3} M), interferon (IFN)α (100 U/ml) for 18 h, the levels of replication of HCV replicon were assessed by luciferase assay. Moreover, cells were cultured

with chloroquine (10^{-5} M) and/or IFNα (100 U/ml) for 7 days, then continued to incubate without drugs for another 21 days. Replication levels of HCV replicon were determined by luciferase assay at 7th and 21st days from cessation of drugs.

Identification of autophagosomes

Naïve Huh7 cells, Huh7/Rep-Feo cells, and Huh7/Rep-Feo treated with IFNα for 14 days were seeded on 30 mm dishes and incubated for 48 h. In addition, Huh7/Rep-Feo cells were treated with chloroquine (10^{-5} M) for 18 h. Cells were prefixed with 2% glutaraldehyde, post-fixed with 1% osmic acid, dehydrated in graded ethanol, embedded in resin, and cut into sections on an ultramicrotome. The cells were analyzed by a transmission electron microscope (Hitachi H7100, Japan). The number of autolysosomes in 100 μm^2 of cytoplasm was counted by using transmission electron microscopy.

Small interfering RNA knockdown of ATG5, 7, LC-3

A combination of four chemically synthesized siRNA duplex molecules targeted to the human ATG5, 7, LC-3α, LC-3β mRNA sequence (Dharmacon, Lafayette, CO) was transiently transfected (final concentration 50 nM) into Huh7/Rep-Feo cells using a transfection reagent (Dharmacon, Lafayette, CO). siRNA targeted to enhanced green fluorescence protein was used as a control. Forty-eight hours after transfection, levels of HCV replication were analyzed by luciferase assay.

Western blot analysis

Twenty-five micrograms of total cell lysates were subjected to SDS/PAGE on a 10% gradient gel and electrophoretically transferred onto polyvinylidene fluoride membranes. After blocking with 5% non-fat dry milk in Tris-buffered saline, membranes were incubated with primary rabbit monoclonal antibody against Phospho-protein kinase R (P-PKR) (Cell Signaling Technology, Danvers, MA) or light-chain 3 (LC3), followed by a secondary horseradish peroxidase (HRP)-conjugated anti-rabbit IgG antibody (Cell Signaling Technology, Danvers, MA). Subsequently, specific bands were visualized using ECL detection kit (Amersham Pharmacia Biotech, Midland, ON, Canada).

Protein degradation assay

Long lived protein is mainly degraded by autophagy [24]. Cells were incubated with Williams' E/10% FBS containing 0.5 μCi/ml [^{14}C]leucine for 24 h to label long-lived proteins. Cells were washed with Williams' E/10% FBS containing 10^{-5} M of unlabeled leucine and incubated with the medium for 2 h to allow degradation of short-lived proteins and minimize the incorporation of labeled leucine. The cells were then washed with phosphate-buffered saline (PBS) and incubated at 37°C with Williams' E/10% FBS in the presence or absence of chloroquine (10^{-5} M). After 4 h, aliquots of the medium were taken and a one-tenth volume of 100% trichloroacetic acid was added to each aliquot. The mixtures were centrifuged at 12,000*g* for 5 min, and the acid-soluble radioactivity was determined using a liquid scintillation counter. At the end of the experiment, the cultures were washed twice with PBS, and 1 ml of cold trichloroacetic acid was added to fix the cell proteins. The fixed cell monolayers were washed with trichloroacetic acid and dissolved in 1 ml of 1 N NaOH at 37°C. Radioactivity in an aliquot of 1 N NaOH was determined by liquid scintillation counting. The percentage of protein degradation was calculated according to published procedures [25].

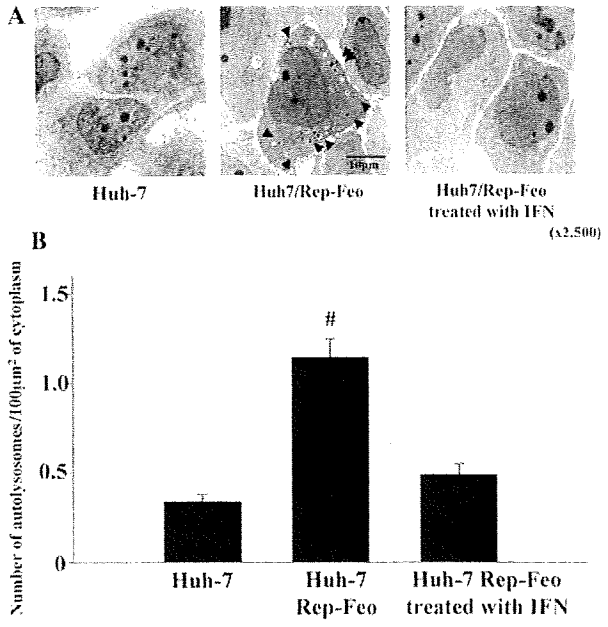

Fig. 1 Expression of autophagy is changed by presence or absence of HCV replicon. **a** Naïve Huh7 cells, Huh7/Rep-Feo cells, and Huh7/Rep-Feo treated with IFNα for 14 days were seeded on 30 mm dishes and incubated for 48 h. The cells were analyzed by a transmission electron microscopy. Autophagosomes (*arrow heads*) were detected by transmission electron microscopy. **b** The number of autolysosomes in 100 μm^2 of cytoplasm was counted by using transmission electron microscopy

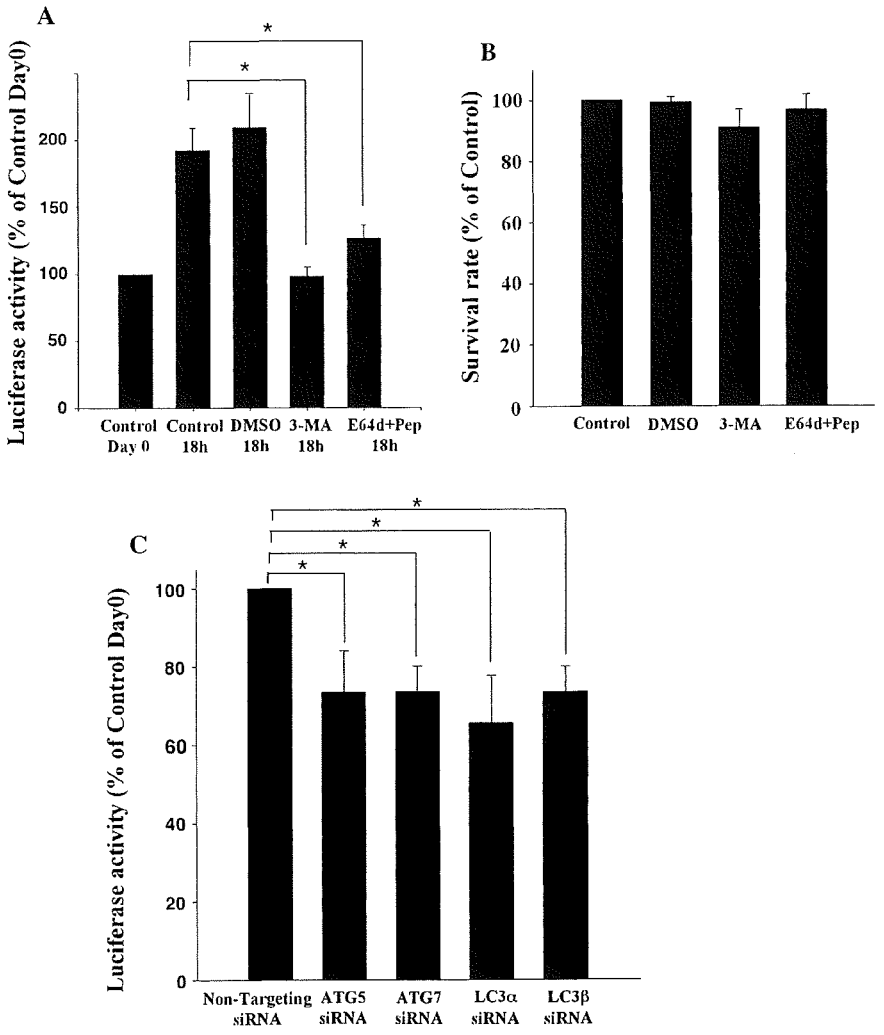

Fig. 2 Inhibition of autophagy suppressed replication of HCV replicon. **a** Cells were treated with 3-methyladenine (3-MA) (10 mM) or a mixture of E64d (1 μg/ml) and pepstatin A (Pep) (1 μg/ml) for 18 h, the levels of replication of HCV replicon were assessed by luciferase assay. **b** Cells were treated with 3-methyladenine (10 mM), mixture of E64d (1 μg/ml) and pepstatin A (1 μg/ml) for 18 h. Cell proliferation reagent WST-1 was added to each well, and the cells were incubated for 1 more hour at 37°C. The absorbance was measured against a background control by microplates reader at 450 nm. The reference wavelength was 650 nm. **c** A combination of four chemically synthesized siRNA duplex molecules targeted to the human ATG5, 7, LC-3α, LC-3β mRNA sequence was transiently transfected into Huh7/Rep-Feo cells using a transfection reagent. siRNA targeted to enhanced green fluorescence protein was used as the control. Forty-eight hours after transfection, levels of HCV replication were analyzed by luciferase assay

Statistical analysis

Differences were compared using ANOVA. Basically P values less than 0.05 were considered as statistically significant.

Results

The inhibition of autophagy suppressed replication of HCV replicon

We counted numbers of autophagosome and autolysosome in cells transduced with HCV replicon Rep-Feo by using electron microscopy. Double membrane vesicles with the morphology of autophagosomes were identified at 2.3 vacuoles/cells in naïve Huh-7 cells, while transfection of HCV replicon increased the number of vacuoles to about fourfold over untransfected Huh-7 cells (Fig. 1a, b). Subsequent treatment of the cells with IFNα (100 U/ml) for 14 days to eliminate HCV replicon substantially decreased the autophagolysosome in cytoplasm of Huh7/Rep-Feo cells (Fig. 1a, b). These observations suggested that HCV replicon induces formation of autophagosomes. To clarify the role of autophagy on the replication of HCV, Huh7/Rep-Feo cells were treated with 3-methyladenine (10 mM) or a mixture of E64d (10 μg/ml) and pepstatin A (10 μg/ml) which inhibited autophagic protein degradation. Replication level of HCV replicon in cells was increased to about twofold after 18 h in control media, however incubation with 3-methyladenine completely blunted increases in replication of HCV replicon. Treatment with 3-methyladenine decreased the number of autophagosomes to about 19% of Huh7/Rep-Feo cells. Furthermore co-incubation with E64d and pepstatin A decreased replication of HCV replicon to about 66% of control (Fig. 2a). Next, WST-1 assay was performed to check the cytotoxicity of these drugs. Treatment with 3-methyladenine or a mixture of

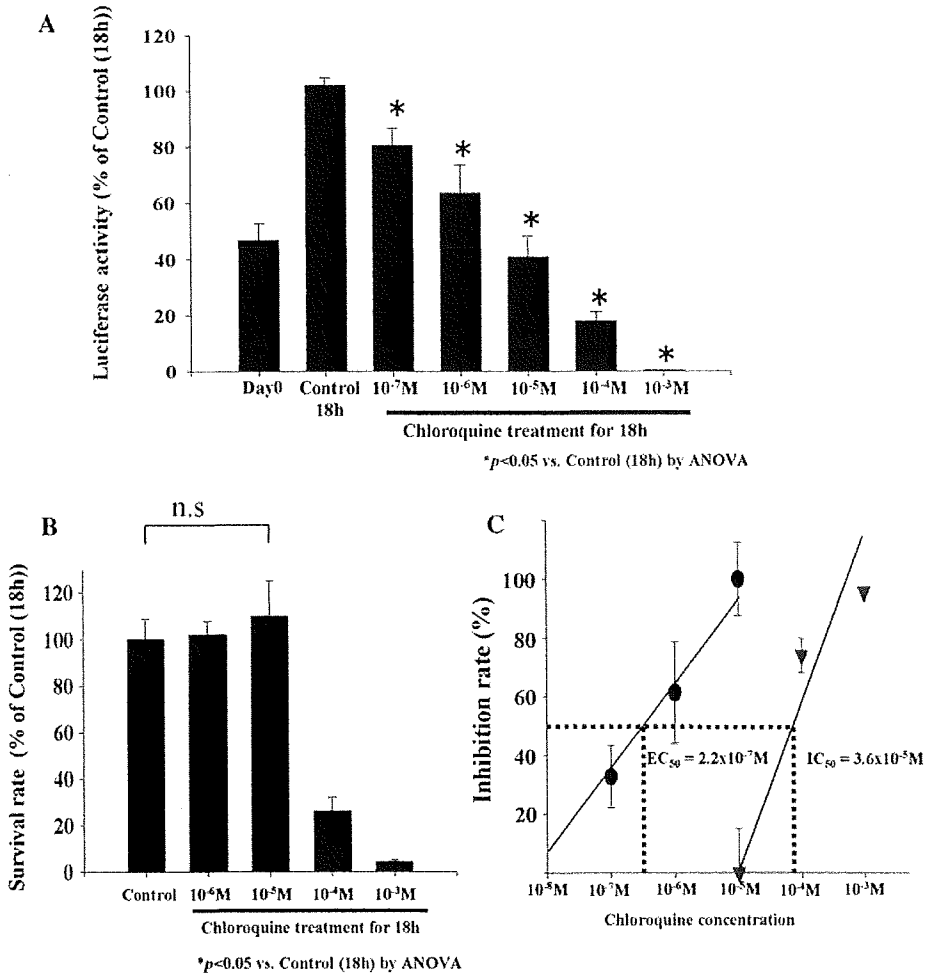

Fig. 3 Effect of chloroquine on inhibition of HCV replication and cell viability. **a** Effect of chloroquine on replication of HCV replicon. Huh-7 Rep/Feo cells were seeded in 48-well plate and incubated with chloroquine (10^{-7}–10^{-3} M) for 18 h. Replication levels of HCV replicon were determined by luciferase assay. Values are shown as percentages of the control cells. [$^*P < 0.05$ vs. control (18 h) by ANOVA]. **b** Effect of chloroquine on proliferation of Huh-7 Rep/Feo cell lines in vitro. Cells seeded in 96-well plates were treated with 10^{-6} to 10^{-3}M of chloroquine. After 18 h, effects on cell proliferation were determined by WST-1 assay. [$^*P < 0.05$ vs. control (18 h) by ANOVA]. **c** Calculation of EC_{50} and IC_{50}. Concentration of chloroquine inhibiting 50% of the replication of HCV replicon is showed as EC_{50}. IC_{50} is the concentration of chloroquine which inhibits 50% of the cell proliferation of Huh-7 Rep/Feo cells

E64d and pepstatin A did not affect cell viability (Fig. 2b). To clarify the role of autophagy induction in the replication of HCV, we suppressed the induction of autophagy by silencing autophagy-related genes (ATG5, ATG7, LC-3α and LC-3β) by siRNA transfection. Silencing of autophagy-related genes reduced the replication of HCV replicon to about 70% of control (Fig. 2c). Transfection with siRNA of autophagy related genes decreased the number of autophagosomes to about 30% of control. These results indicated that autophagy plays a pivotal role in replication of HCV.

Chloroquine inhibits the replication of HCV replicon

Next, we evaluated the anti-HCV effect of chloroquine, which is a lysosomotropic agent that raises intralysosomal pH and impairs autophagic protein degradation. To assess the effects of chloroquine on the intracellular replication of the HCV replicon, Huh7/Rep-Feo cells were cultured with various concentrations of chloroquine in the medium. The replication of the HCV replicon was increased to about twofold within 18 h in the control media, however, which was suppressed by chloroquine in a dose-dependent manner (Fig. 3a). Next, cytotoxicity of chloroquine was analysed by WST-1 assays. Huh7/Rep-Feo cells treated with chloroquine showed no significant effect on cell viability in doses of lower than 10^{-5} M (Fig. 3b). However, incubation with 10^{-4} M of chloroquine reduced the cell viability to 25% of control. On the basis of the toxicity curve, the IC_{50} of the drug was calculated to be 3.6×10^{-5} M (Fig. 3c). The average EC_{50} of chloroquine was calculated as 2.2×10^{-7} M (Fig. 3c). The replication of HCV replicon was suppressed to nearly 40% of control at 10^{-5} M of chloroquine, which did not affect cell viability. These data indicated that chloroquine efficiently inhibited the replication of HCV replicon in the absence of toxic effect to cells at the concentration of 10^{-5} M. Accordingly, we used 10^{-5} M of chloroquine for the following study.

Next, we conducted the following assay to determine the synergistic inhibitory effect of chloroquine to IFNα on HCV replication. Treatment with chloroquine for 18 h

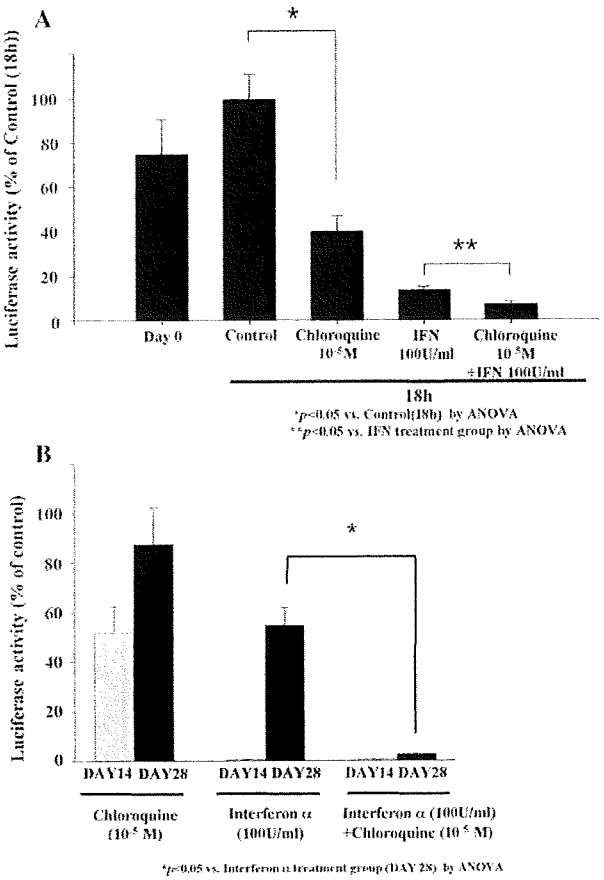

Fig. 4 Combination effect of chloroquine with IFNα on HCV replication. **a** Huh-7 Rep/Feo cells were treated with chloroquine (10^{-5} M) and/or IFNα (100 U/ml) for 18 h. Values are shown as percentages of the control cells [$^{*}P < 0.05$ vs. control (18 h) by ANOVA, $^{**}P < 0.05$ vs. IFNα treatment group by ANOVA]. **b** Assessment of re-propagation of HCV replicon after long term treatment of chloroquine and/or IFNα. Huh-7 Rep/Feo was incubated with chloroquine (10^{-5} M) and/or IFNα (100 U/ml) for 7 days, then drugs were removed from the medium and incubation continued for another 21 days. Luciferase assay was performed at the 7th and 21st days from cessation of drugs. Values are shown as percentages of the control cells [$^{*}P < 0.05$ vs. IFNα treatment group (day 28) by ANOVA]

resulted in a significant decrease of HCV replicon to about 40% of control. On the other hand, incubation with IFNα for 18 h inhibited the replication of HCV replicon to the levels about 15% of controls as expected. However, co-incubation with 100U/ml of IFNα and 10^{-5} M of chloroquine further decreased HCV replication significantly (Fig. 4a).

To determine whether long-term chloroquine treatment inhibits post-treatment re-propagation of HCV replicon, we followed up luciferase activity of the cells at the 7th and 21st days after 7 days of treatment with chloroquine and/or IFNα (Fig. 4b). In HCV replicon cells treated by chloroquine, luciferase activities recovered to 53 and 88% on 7 and 21 days after cessation of treatment. In cells that were treated by IFNα, luciferase activity maintained background level for 7 days post-treatment. However, it reappeared in 21 days. In sharp contrast, co-incubation with IFNα and chloroquine for 7 days suppressed HCV replication for the extensive period up to 21 days, even in the absence of these drugs (Fig. 4b).

Anti-HCV effect of chloroquine independent of IFN signaling pathway

IFN-inducible double-stranded RNA-activated protein kinase R (PKR) plays a key antiviral role against hepatitis C virus [26, 27]. To elucidate the mechanisms of the inhibitory effect of chloroquine on HCV replication, phosphorylated PKR (P-PKR) was evaluated by western blotting analysis. P-PKR was detectable in cells treated with IFNα after 24 h; this increase in P-PKR expression peaked at 24 h after IFNα treatment and was reduced at 48 h (Fig. 5a). In contrast, P-PKR was not observed in cells treated with chloroquine at any time point.

Chloroquine blunts autophagic proteolysis in cells transfected with HCV replicon

It is reported that chloroquine disrupts lysosomal function, preventing effective autophagic protein degradation, leading to the accumulation of ineffective autophagosomes [28]. Therefore, we investigated if chloroquine led to the accumulation of autolysosomes as a result of suppression of proteolysis. We performed electron microscopic investigation to evaluate quantities of autophagosomes and autolysosomes. Ultrastructural analysis identified 0.94 ± 0.1 vacuoles/100 μm^2 of autolysosomes in control cells; however, treatment with chloroquine increased the number of autolysosomes dramatically to about 13-fold over control (Fig. 5b). Furthermore, the molecular form of LC3 protein of the cells, which is a component of autophagosomes, was examined by western blot analysis to ensure that chloroquine treatment leads to the accumulation of autophagosomes and autolysosomes. As shown in Fig. 5c, immunopositive protein bands for LC3-I and LC3-II forms were clearly evident in control cells. After chloroquine treatment, LC3-II expression increased at 4 h (Fig. 5c) to about threefold over control without enhancing LC3-I expression, and at 8 h (Fig. 5c) LC3-II expression was further enhanced. Finally, we evaluated turnover of the long-lived protein leucine, which was mainly degraded by autophagy. Huh7/Rep-Feo cells were labeled with [^{14}C]leucine for 24 h, and degradation of [^{14}C]leucine in cells treated with or without chloroquine was measured. Chloroquine treatment decreased degradation of leucin to 76% of control, indicating that chloroquine blunts degradation of proteins via an autophagic

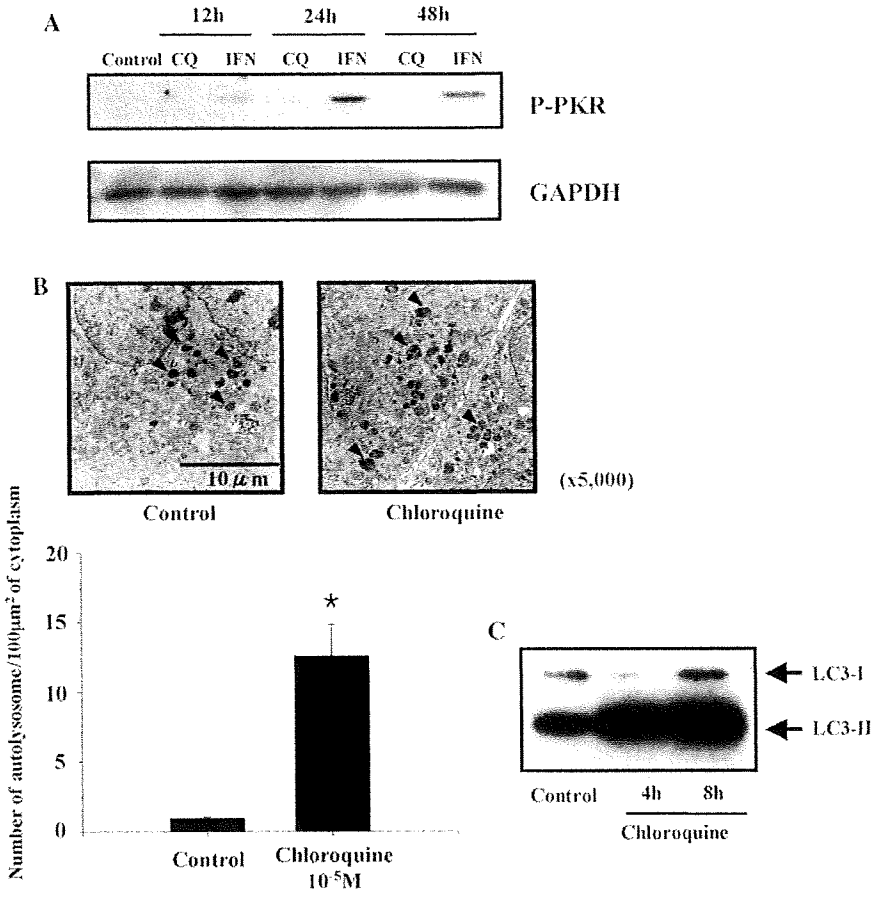

Fig. 5 Chloroquine suppresses autophagic protein degradation, not interferon pathways. **a** Cells were treated with 10^{-5} M of chloroquine (CQ) or 100 U/ml of IFNα for 24–48 h. Phosphorylation of PKR was assessed by western blot analysis. GAPDH was used as loading control. **b** Ultrastructural analysis showing the effect of chloroquine on the number of autolysosomes. Huh-7/Rep-Feo cells were incubated with chloroquine for 18 h. Autolysosomes were identified as the double membrane vesicles (arrow heads) of cytoplasm in Huh-7 Rep/Feo. The number of autolysosomes in 100 μm^2 of cytoplasm was counted by using transmission electron microscopy. Data represent mean ± SEM of individual preparations from pictures (*$P < 0.05$ vs. control by ANOVA). **c** Western blot analysis of LC3 in Huh7 Rep/Feo. The lysate of Huh7 Rep/Feo treated with chloroquine for 4–8 h were immunoblotted with LC3. GAPDH was used as loading control

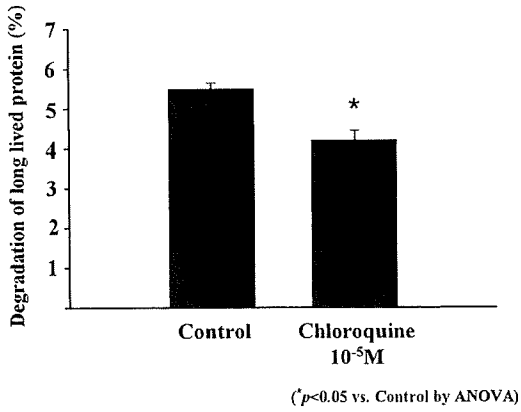

Fig. 6 Turnover of long lived protein. Huh-7 Rep/Feo cells were labeled with [^{14}C]leucin for 4 h, then degradation of long-lived protein in chloroquine treated cells was measured as described in Materials and Methods. The percentage of protein degradation was calculated by dividing the amount of acid-soluble radioactivity in the medium at that time by the amount of acid-precipitable radioactivity present in the cells at time zero. Data are mean ± SEM of value of triplicate in each group (*$P < 0.05$)

pathway (Fig. 6). These results demonstrate that chloroquine-induced the accumulation of autolysosomes was due to disruption of autophagic proteolysis.

Discussion

Previous reports have disclosed that autophagy plays a pivotal role on the replication of several RNA viruses [10–12]. Our present results demonstrate that autophagy is induced by transfection of HCV replicon and is reduced by deletion of replicon due to IFNα (Fig. 1a, b). These results suggest that autophagy is induced in the presence of HCV replication in its host cells. However, the role of autophagy in the pathogenesis of HCV is largely unclear. We found that the inhibition of autophagosome formation and autophagic proteolysis blunt the replication of genotype 1b subgenomic HCV replicon (Fig. 2a, c). Sir et al. [13] reported that inhibition of autophagy also reduced the replication of the JFH1-based full length genotype 2a genome. Therefore, the utilization of autophagy on viral replication is shown by HCV strains across different genotypes.

On the other hand, not only a silencing of autophagic gene but also pharmacological inhibition of autophagic proteolysis possesses anti-HCV effects (Fig. 2a, c). However, treatment with both chloroquine and the mixture of E64d and pepstatin induced the accumulation of

autophagosomes in cytoplasm. Therefore, it is likely that HCV does not utilize the double membrane structure as the localization of the viral replication formation. These results support the hypothesis that protein degradation due to autophagy is important for HCV replication.

Chloroquine is a well-known inhibitor of autophagic protein degradation and is often used as an anti-malarial agent. Moreover, the anti-viral effect of chloroquine on other RNA viruses has been already reported in clinical trials [15, 16]. In our results, chloroquine inhibits the intracellular replication of an HCV replicon in a dose-dependent manner (Fig. 3a). This antiviral effect of chloroquine was clearly not due to cytotoxic effects (Fig. 3b). Moreover, chloroquine possesses a synergistic effect with IFNα on HCV replication (Fig. 4a). Although IFNα possesses strong anti-HCV effects, re-propagation of HCV replicon was observed after 3 weeks following 7 days of treatment with IFNα. Interestingly, co-incubation with IFNα and chloroquine for 7 days prevented re-propagation of HCV replicon (Fig. 4b). Chloroquine is a lysosomal weak base that is known to affect acid vesicles leading to dysfunction of several proteins [29]. It was demonstrated that disruption of lysosomal function impairs maturation of viruses through inhibiting the low-pH dependent proteases in trans-Golgi vesicles in HIV and the SARS coronavirus infection in vitro [15, 29]. However, little is understood about the mechanism of its antiviral effect. In previous reports, various drugs which possess inhibitory effects on the replication of HCV and have a synergistic action with IFNα have been proposed as new therapeutic agents to treat HCV. Some of them have proved to exhibit their anti-HCV effects through augmentation of IFN-induced antiviral gene responses [30, 31]. However, the anti-HCV effect of chloroquine was not associated with activation of one of IFN receptors signaling molecule PKR (Fig. 5a). Our results showed chloroquine induced the accumulation of ineffective autophagosomes in cytoplasm of Huh7/Rep-Feo cells (Fig. 5b) and inhibited the degradation of long-lived protein leucine (Fig. 6). These findings imply that chloroquine effectively impairs the function of autophagy in our experiment. These results indicated that chloroquine is a new anti-HCV agent that targets the autophagic proteolysis.

Previous reports have shown that chloroquine possesses anti-viral effects on various RNA viruses. Its best-studied effects are those against HIV replication, which are being tested in clinical trials [17, 18]. HCV co-infection is common in HIV-positive patients in USA and Europe [32, 33]. Since HIV infection accelerates the progression of HCV-related liver disease, treatment of HCV is generally recommended. However, co-infected patients have a greater risk of antiretroviral therapy-associated hepatotoxicity than patients with HIV only [34]. Moreover, treatment with ribavirin is believed to increase the risk of anemia in patients taking the HIV drug zidovudine [35]. A clinical study designed for HIV patients showed the safety and efficacy of chloroquine used for long terms up to 48 weeks [36]. Therefore, the combination therapy of interferon and chloroquine is, possibly, a hopeful therapy for HCV–HIV co-infected patients. Since chloroquine is known as one of the inexpensive drugs, therefore, chloroquine might provide a new effective, safe and economical therapeutic option for patients with HCV. In conclusion, autophagic proteolysis might be a new therapeutic target on the replication of HCV.

References

1. Yotsuyanagi H, Koike K. Drug resistance in antiviral treatment for infections with hepatitis B and C viruses. J Gastroenterol. 2007;42:329–35.
2. Bruno S, Stroffolini T, Colombo M, Bollani S, Benvegnù L, Mazzella G, et al. Sustained virological response to interferon-alpha is associated with improved outcome in HCV-related cirrhosis: a retrospective study. Hepatology. 2007;45:579–87.
3. Shiffman ML, Cooksley WG, Dusheiko GM, Lee SS, Balart L, Reindollar R, et al. Peginterferon alfa-2a in patients with chronic hepatitis C and cirrhosis. N Engl J Med. 2000;343:1673–80.
4. Sezaki H, Suzuki F, Kawamura Y, Yatsuji H, Hosaka T, Akuta N, et al. Poor response to pegylated interferon and ribavirin in older women infected with hepatitis C virus of genotype 1b in high viral load. Dig Dis Sci. 2009;54:1317–24.
5. Honda T, Katano Y, Urano F, Murayama M, Hayashi K, Ishigami M, et al. Efficacy of ribavirin plus interferon-α in patients aged 60 years with chronic hepatitis C. J Gastroenterol Hepatol. 2007;22:989–95.
6. Wang CW, Klionsky DJ. The molecular mechanism of autophagy. Mol Med. 2003;9:65–76.
7. Klionsky DJ, Emr SD. Autophagy as a regulated pathway of cellular degradation. Science. 2000;290:1717–21.
8. Reggiori F, Klionsky DJ. Autophagy in the eukaryotic cell. Eukaryot Cell. 2002;1:11–21.
9. Prentice E, Jerome WG, Yoshimori T, Mizushima N, Denison MR. Coronavirus replication complex formation utilizes components of cellular autophagy. J Biol Chem. 2004;279:10136–41.
10. Randolph VB, Winkler G, Stollar V. Acidotropic amines inhibit proteolytic processing of flavivirus prM protein. Virology. 1990;174:450–8.
11. Posthuma CC, Pedersen KW, Lu Z, Joosten RG, Roos N, Zevenhoven-Dobbe JC, et al. Formation of the arterivirus replication/transcription complex: a key role for nonstructural protein 3 in the remodeling of intracellular membranes. J Virol. 2008;82:4480–91.
12. Suhy DA, Giddings TH Jr, Kirkegaard K. Remodeling the endoplasmic reticulum by poliovirus infection and by individual viral proteins: an autophagy-like origin for virus-induced vesicles. J Virol. 2000;74:8953–65.
13. Sir D, Chen WL, Choi J, Wakita T, Yen TS, Ou JH. Induction of incomplete autophagic response by hepatitis C virus via the unfolded protein response. Hepatology. 2008;48:1054–61.

14. Poole B, Ohkuma S. Effect of weak bases on the intralysosomal pH in mouse peritoneal macrophages. J Cell Biol. 1981;90: 665–9.
15. Vincent MJ, Bergeron E, Benjannet S, Erickson BR, Rollin PE, Ksiazek TG, et al. Chloroquine is a potent inhibitor of SARS coronavirus infection and spread. Virol J. 2005;2:69.
16. Savarino A, Gennero L, Chen HC, Serrano D, Malavasi F, Boelaert JR, et al. Anti-HIV effects of chloroquine: mechanisms of inhibition and spectrum of activity. AIDS. 2001;15:2221–9.
17. Savarino A, Boelaert JR, Cassone A, Majori G, Cauda R. Effects of chloroquine on viral infections: an old drug against today's diseases? Lancet Infect Dis. 2003;3:722–7.
18. Sperber K, Chiang G, Chen H, Ross W, Chusid E, Gonchar M, et al. Comparison of hydroxychloroquine with zidovudine in asymptomatic patients infected with human immunodeficiency virus type 1. Clin Ther. 1997;19:913–23.
19. Paton NI, Aboulhab J. Hydroxychloroquine, hydroxyurea and didanosine as initial therapy for HIV-infected patients with low viral load: safety, efficacy and resistance profile after 144 weeks. HIV Med. 2005;6:13–20.
20. Tanabe Y, Sakamoto N, Enomoto N, Kurosaki M, Ueada E, Maekawa S, et al. Synergistic inhibition of intracellular hepatitis C virus replication by combination of ribavirin and interferon-alpha. J Infect Dis. 2004;189:1129–39.
21. Yokota T, Sakamoto N, Enomoto N, Tanabe Y, Miyagishi M, Maekawa S, et al. Inhibition of intracellular hepatitis C virus replication by synthetic and vector-derived small interfering RNAs. EMBO Rep. 2003;4:602–8.
22. Seglen PO, Gordon PB. 3-Methyladenine: specific inhibitor of autophagic/lysosomal protein degradation in isolated rat hepatocytes. Proc Natl Acad Sci USA. 1982;79:1889–92.
23. Ueno T, Ishidoh K, Mineki R, Tanida I, Murayama K, Kadowaki M, et al. Autolysosomal membrane-associated betaine homocysteine methyltransferase. Limited degradation fragment of a sequestered cytosolic enzyme monitoring autophagy. J Biol Chem. 1999;274:15222–9.
24. Klionsky DJ, Emr SD. Autophagy as a regulated pathway of cellular degradation. Science. 2000;290:1717–21.
25. Gronostajski RM, Pardee AB. Protein degradation in 3T3 cells and tumorigenic transformed 3T3 cells. J Cell Physiol. 1984;119:127–32.
26. Clemens MJ. PKR–a protein kinase regulated by double-stranded RNA. Int J Biochem Cell Biol. 1997;29:945–9.
27. Gale MJ Jr, Korth MJ, Tang NM, Tan SL, Hopkins DA, Dever TE, et al. Evidence that hepatitis C virus resistance to interferon is mediated through repression of the PKR protein kinase by the nonstructural 5A protein. Virology. 1997;230:217–27.
28. Glaumann H, Ahlberg J. Comparison of different autophagic vacuoles with regard to ultrastracture, enzymatic composition, and degradation capacity—formation of crinosomes. Exp Mol Pathol. 1987;47:346–62.
29. Thorens B, Vassalli P. Chloroquine and ammonium chloride prevent terminal glycosylation of immunoglobulins in plasma cells without affecting secretion. Nature. 1986;321:618–20.
30. Dev A, Patel K, McHutchison JG. New therapies for chronic hepatitis C virus infection. Curr Gastroenterol Rep. 2004;6:77–86.
31. Lin K, Kwong AD, Lin C. Combination of a hepatitis C virus NS3-NS4A protease inhibitor and alpha interferon synergistically inhibits viral RNA replication and facilitates viral RNA clearance in replicon cells. Antimicrob Agents Chemother. 2004;48:4784–92.
32. Staples CT Jr, Rimland D, Dudas D. Hepatitis C in the HIV (human immunodeficiency virus) Atlanta V.A. (Veterans Affairs Medical Center) Cohort Study (HAVACS): the effect of coinfection on survival. Clin Infect Dis. 1999;29:150–4.
33. Denis F, Adjide CC, Rogez S, Delpeyroux C, Rogez JP, Weinbreck P. Seroprevalence of HBV, HCV and HDV hepatitis markers in 500 patients infected with the human immunodeficiency virus. Pathol Biol (Paris). 1997;45:701–8.
34. Sulkowski MS, Benhamou Y. Therapeutic issues in HIV/HCV-coinfected patients. J Viral Hepat. 2007;14:371–86.
35. Alvarez D, Dieterich DT, Brau N, Moorehead L, Ball L, Sulkowski MS. Zidovudine use but not weight-based ribavirin dosing impacts anaemia during HCV treatment in HIV-infected persons. J Viral Hepat. 2006;13:683–9.
36. Paton NI, Aboulhab J, Karim F. Hydroxychloroquine, hydroxycarbamide, and didanosine as economic treatment for HIV-1. Lancet. 2002;359:1667–8.

J Gastroenterol 2009; 44:173–182
DOI 10.1007/s00535-008-2284-4

Journal of Gastroenterology

© Springer 2009

Musashi-1 suppresses expression of Paneth cell-specific genes in human intestinal epithelial cells

Minekazu Murayama[1]*, Ryuichi Okamoto[1,2]*, Kiichiro Tsuchiya[1], Junko Akiyama[1]
Tetsuya Nakamura[1,2], Naoya Sakamoto[1], Takanori Kanai[1], and Mamoru Watanabe[1]

[1]Department of Gastroenterology and Hepatology, Graduate School, Tokyo Medical and Dental University, 1-5-45 Yushima, Bunkyo-ku, Tokyo 113-8519, Japan
[2]Department of Advanced Therapeutics in GI Diseases, Graduate School, Tokyo Medical and Dental University, Tokyo, Japan

Background. Musashi-1 (Msi-1) is a RNA-binding protein, known as a putative marker of intestinal stem cells (ISCs). However, little is known about the function of Msi-1 within human intestinal epithelial cells (IECs). Thus, the present study aimed to clarify the role of Msi-1 in differentiation and proliferation of IECs. ***Methods.*** A human intestinal epithelial cell line stably expressing Msi-1 was established. Proliferation of the established cell lines was measured by bromodeoxyuridine incorporation, whereas differentiation were assessed by reverse transcriptase-polymerase chain reaction (RT-PCR) analysis of lineage-specific genes. Activities of the Notch and Wnt pathways were examined either by reporter assays or expression of downstream target genes. The distribution of Msi-1 and PLA2G2A expression in vivo was determined by immunohistochemistry. ***Results.*** Constitutive expression of Msi-1 in IECs had no significant effect on cell proliferation, but suppressed expression of Paneth cell-specific genes, including *PLA2G2A*. Msi-1 appeared to suppress expression of the *PLA2G2A* gene at the mRNA level. Analysis of Notch and Wnt pathway activity, however, revealed no significant change upon Msi-1 expression. The expression of Msi-1 and PLA2G2A in vivo was restricted to IECs residing at the lowest part of the human intestinal crypt, but was clearly separated to within basal columnar cells or mature Paneth cells, respectively. ***Conclusions.*** Msi-1 suppresses expression of Paneth cell-specific genes in IECs, presumably through a pathway independent from Notch or Wnt. These findings suggest Msi-1 is a negative regulator of Paneth cell differentiation, an may contribute to maintain the undifferentiated phenotype of ISCs.

Key words: Musashi-1, intestinal epithelial cells, Paneth cells, PLAG2A

Introduction

The rapid and continuous renewal of the intestinal epithelium is maintained by the regulated supply of newborn cells that arise from a common progenitor cell called the intestinal stem cell (ISC).[1] Such tissue-specific stem cells share common potentials to self renew and also to give rise to all cell lineages composing the residing tissue.[2] Such properties of stem cells are maintained by a complex interaction of various cell-signaling pathways.[3] Among such signaling pathways, Wnt and Notch represent the core molecular pathways that play crucial roles in maintaining stem cell properties.[4] Indeed, both Wnt and Notch signaling have been shown to function in intestinal crypt epithelial cells, including the ISCs.[5] A recent study identified Lgr-5, a direct target of the canonical Wnt pathway, as a definite marker of murine ISCs.[6] This study further emphasized the dominant role of the canonical Wnt pathway in maintaining cell proliferation and multipotency of ISCs. It is, however, known that activation of the canonical Wnt pathway is present not only in ISCs but also in Paneth cells residing just adjacent to ISCs, where it promotes maturation and restricts the cell position of such cells.[7] Thus, activation of the canonical Wnt pathway appears to have a completely different function in ISCs and Paneth cells, presumably depending on the cell context determined by other molecular factors. However, the molecular mechanism regulating such lineage-specific functions of canonical Wnt signaling in IECs remains largely unknown.

Musashi-1 (Msi-1) is an RNA-binding protein, and its gene was formerly reported as another candidate marker gene for ISCs.[8,9] Its molecular function has been deter-

Received: July 22, 2008 / Accepted: August 16, 2008
Reprint requests to: K. Tsuchiya
*These authors contributed equally to this work.

mined as translational repression of target genes, such as *m-Numb*, a negative regulator of Notch signaling.[10] In both mice and humans, Msi-1 has been shown to be expressed in ISCs, but in sharp contrast, its expression is completely lacking in mature Paneth cells.[8,9,11] Thus, Msi-1 might function within intestinal epithelial cells (IECs) to maintain their undifferentiated state.[12,13] However, the molecular function of Msi-1 in IECs has never been described.

Herein, we show that expression of Msi-1 in IECs suppressed expression of Paneth cell-specific genes, such as *PLA2G2A*. Msi-1 appeared to downregulate expression of the *PLA2G2A* gene at the mRNA level, through a molecular pathway independent of both Notch and Wnt, the two major molecular pathways that are known to regulate Paneth cell differentiation. These results suggest that Msi-1 is a negative regulator of Paneth cell differentiation in IECs, and that it has a functional role in maintaining the undifferentiated state of ISCs.

Materials and methods

Cell culture

Human colon cancer-derived LS174T cells were cultured in minimal essential medium (GIBCO, Billings, MT, USA) supplemented with 10% fetal bovine serum, 2 mM L-glutamine, 100 U/ml penicillin, and 100 mg/ml streptomycin (Invitrogen, Carlsbad, CA, USA), at 37°C in a humidified incubator with 5% CO_2.

Plasmids

For construction of the expression plasmid for Msi-1 (pcDNA3.0-Msi-1), the entire coding lesion of the mouse *Msi-1* gene was polymerase chain reaction (PCR) amplified from pcDNA3.0-FLAG-Msi-1 (kindly provided by Dr. Hideyuki Okano), and inserted into pcDNA3.0 (Invitrogen). For construction of the enhanced green fluorescent protein (EGFP) expression plasmid (pCMV-FLAG-EGFP), the coding sequence of pEGFP-C1 (Stratagene, La Jolla, CA, USA) was PCR amplified and inserted into the pCMV-FLAG-Tag vector (Stratagene).

Establishment of cell lines stably expressing Msi-1 or EGFP

Expression plasmids for Msi-1 (pcDNA3.0-Msi-1) or EGFP (pCMV-FLAG-EGFP) were transfected into LS174T cells as previously described.[14] After 2 days of culture, cells were selected by addition of G418 (1 mg/ml) to the culture medium. Subsequently, G418-resistant cells were cloned into sublines expressing Msi-1 or EGFP, designated as LS174T/Msi-1 cells or LS174T/GFP cells, respectively.

Microscopic imaging and immunostaining of cultured cells

Microscopic images of cultured cells were collected using an epifluorescence microscope system (BZ-2000, Keyence, Osaka, Japan). Immunostaining of cultured cells were done as previously described.[15,16] For detection of Musashi-1, primary antibody (14H1, kindly provided by Dr. Hideyuki Okano) was diluted to 1:1000 and detected by an Alexa-488-conjugated secondary antibody (Molecular Probes, Eugene, OR USA). Cells were counterstained by 4′,6-diamino-2-phenylindole (DAPI), and mounted in Vectashield mounting medium (Vector Laboratories, Burlingame, CA, USA).

Cell proliferation assay

Incorporation of bromodeoxyuridine (Brd-U) was examined using a cell proliferation enzyme-linked immunosorbent assay (ELISA) kit (Roche Diagnostics, Mannheim, Germany), according to the manufacturer's instructions. Briefly, cells were seeded onto a 96-well dish at various cell densities, cultured for 48 h, and labeled with Brd-U for 8 h at the end of culture. Each condition was measured in triplicate and the results analyzed by Student's *t* test.

Reverse transcription-polymerase chain reaction

Total RNA was prepared using TRIzol reagent (Invitrogen) according to the manufacturer's instructions. Reverse transcription (RT) was carried out as previously described.[15] Forward and reverse primers used for the PCR reaction are summarized in Table 1. For semiquantitative PCR, 1 µl of cDNA was amplified with 0.25 U of LA *Taq* polymerase (Takara, Otsu, Japan), using the optimized amplification cycles determined for each primer set. Amplified products were separated by 1.8% agarose gel electrophoresis, stained with ethidium bromide, and visualized by the Lumi-Imager F1 system (Roche Diagnostics). For quantitative PCR, 1 µl of cDNA was amplified using SYBR green master mix (Qiagen, Valencia, CA, USA), and analyzed by a 7500 real-time PCR system (Applied Biosystems, Foster City, CA, USA).

Immunoblotting

Immunoblot analysis was done as previously described.[15] Briefly, 1×10^6 cells were seeded onto 6-cm culture dishes and collected for protein extraction after 48 h of

Table 1. Primers used in the present study

Gene	Primer sequence	
	Forward	Reverse
Musashi-1	5′-GGCTTCGTCACTTTCATGGACCAGGCG-3′	5′-GGGAACTGGTAGGTGTAAC-3′
MUC2	5′-CTGCACCAAGACCGTCCTCATG-3′	5′-GCAAGGACTGAACAAAGACTCAGAC-3′
TFF3	5′-TGAGGAGTACGTGGGCCTGTCTGCAAA-3′	5′-CGGGTGGAGCATGGGACCTTTATT-3′
KLF-4	5′-GGGAGAAGACACTGCGTCA-3′	5′-GGAAGCACTGGGGGAAGT-3′
Isomaltase	5′-TACTAGAAGACAAGATCCCGCT-3′	5′-GTAGTTCCTTTCCCCCATACAT-3′
Lactase	5′-CCCCAAAGCATCAGCGAAGTT-3′	5′- CTACACGTTTCCGCAAGAGCT-3′
PLA2G2A	5′-ACCATGAAGACCCTCCTACTG-3′	5′-GAAGAGGGGACTCAGCAACG-3′
HD-5	5′-CCCAGCCATGAGGACCATCG-3′	5′-TCTATCTAGGAAGCTCAGCG-3′
HD-6	5′-CCACTCCAAGCTGAGGATGATC-3′	5′-CCACTCCAAGCTGAGGATGATC-3′
Lysozyme	5′-CTCTCATTGTTCTGGGGC-3′	5′-ACGGACAACCCTCTTTGC-3′
c-Myc	5′-CTTCTGCTGGAGGCCACAGCAAACCTCCTC-3′	5′-CCAACTCCGGGATCTGGTCACGCAGGG-3′
EphB3	5′-AGCAACCTGGTCTGCAAAGT-3′	5′-TCCATAGCTCATGACCTCCC-3′
G3PDH	5′-TGAAGGTCGGAGTCAACGGATTTGGT-3′	5′-CATGTGGGCCATGAGGTCCACCAC-3′
GFP	5′-TGAAGGTCGGAGTCAACGGATTTGGT-3′	5′-CATGTGGGCCATGAGGTCCACCAC-3′

culture. Total cell lysate was prepared using radioimmunoprecipitation assay buffer. Fifty micrograms of each lysate was subjected to analysis. Primary antibodies used were as follows: mouse anti-Musashi-1 (1:500, Chemicon, Temecula, CA, USA), rabbit anti-GFP (1:2500, MBL, Nagoya, Japan), Goat anti-NUMB (1:100, Santa Cruz Biotechnology, Santa Cruz, CA, USA), rabbit anti-Hes1 (kindly provided by Dr. T. Sudo), mouse anti-β-actin (1:5000, Sigma, St. Louis, MO, USA). Primary antibodies were detected by the appropriate horseradish peroxidase-conjugated secondary antibodies, and visualized by the Lumi-Imager F1 system (Roche Diagnostics) using enhanced chemiluminescence (Amersham Biosciences, Buckinghamshire, UK) as a substrate.

Quantification of PLA2G2A secretion

For PLA2G2A protein quantification, 1×10^6 cells were seeded onto a 6-cm dish and cultured for up to 5 days. Supernatants were collected at 1, 3, and 5 days of culture and analyzed with a sPLA2 (human type IIA) enzyme immunoassay (EIA) kit (Cayman Chemical, Ann Arbor, MI, USA). The assay was performed in triplicate, and the results statistically analyzed by paired Student's *t* test.

Reporter assays

Reporter assays using the dual luciferase system (Promega, Madison, WI, USA) has been previously described.[15] TOP-Flash and FOP-Flash reporter plasmids were purchased from Upstate Biotechnology (Lake Placid, NY, USA). Each condition was examined in triplicate and the results analyzed by Student's *t* test.

Human intestinal tissue specimens

Normal human small intestinal tissues were obtained from patients who underwent surgery for the treatment of Crohn's disease at Yokohama Municipal General Hospital, and macroscopically intact regions of each specimen were subjected for immunohistochemical staining. Written informed consent was obtained from each patient, and the study was approved by the ethics committee of Yokohama Municipal General Hospital and Tokyo Medical and Dental University.

Immunohistochemistry

Immunohistochemistry using human intestinal tissues has been previously described.[11] Primary antibodies used were as follows: Rat anti-Musashi-1 (1:1000, kindly provided by Dr. Hideyuki Okano), and Goat-anti-human PLA2G2A (1:200, sc-14468, Santa Cruz Biotechnology). Microwave treatment (500 W, 10 min) in 10 mM citrate buffer was required for detection of both Msi-1 and PLA2G2A. Msi-1 antibody was visualized using Alexa-488-conjugated Tyramide (Molecular Probes) as a substrate for the avidin–biotin complex (Vector Laboratories), whereas PLA2G2A antibody was visualized by Alexa-594-conjugated secondary antibody (Molecular Probes). Sections were counterstained with DAPI and mounted in Vectashield mounting medium (Vector Laboratories). Fluorescent images were captured by the epifluorescence microscope system (BZ-2000, Keyence).

Results

Establishment of stable cell lines constitutively expressing Msi-1

To analyze the functional role of Msi-1, we planned to assess the effect of Msi-1 expression in human IECs. For this purpose, we employed LS174T cells as the parental (host) cells, as we have previously shown that these cells readily express a wide variety of lineage-specific genes,[15,16] but do not express detectable amount of endogenous Msi-1 protein (Fig. 1B). These features of LS174T cells makes them an ideal model for examining whether expression of Msi-1 can modulate proliferation as well as differentiation of human IECs. Following transfection of an expression plasmid for Msi-1, we successfully generated three clones of LS174T cells that stably expressed Msi-1 (designated hereafter as LS174T/Msi-1 cells). We also generated another clone of LS174T cells that stably expressed EGFP to serve as a control (LS174T/GFP cells). RT-PCR analysis of these generated cell clones revealed mRNA expression from the corresponding transgenes (Fig. 1A). Also, immunoblot analysis clearly showed expression of green fluorescent protein (GFP) or Msi-1 protein in LS174T/GFP or LS174T/Msi-1 cells, respectively (Fig. 1B). An epifluorescence view of these cells also assured constitutive expression of GFP in all of the LS174T/GFP cells but not in the other cell clones (Fig. 1C). In contrast, immunostaining of Msi-1 protein revealed constitutive expression of Msi-1 protein in all of the LS174T/Msi-1 cells but not in the other cell clones (Fig. 1D). A phase-contrast view showed no clear difference between parental cells and LS174T/GFP cells, as both cell clones aggregated to form a round cell colony consisting of vertically piled-up cells (Fig. 1C). LS174T/Msi-1 cells, however, failed to form such cell colonies, but showed a very flat cell morphology and appeared to spread horizontally as a monolayer of cells (Fig. 1C). These results collectively confirmed that the generated cells surely expressed GFP or Msi-1 protein in a constitutive manner, and also suggested that expression of Msi-1 might have induced some intracellular changes influencing the shape and nature of colony formation of LS174T cells.

Expression of Msi-1 did not change cell proliferation but decreased expression of Paneth cell-specific genes in LS174T cells

As we found morphological changes in cells and colony shape of LS174T/Msi-1 cells (Fig. 1C), we examined whether they underwent changes in cell proliferation. Analysis of Brd-U incorporation, however, showed no significant change in LS174T/Msi-1 cells compared with LS174T/GFP cells (Fig. 2A). Next, we analyzed the expression of lineage-specific genes, to evaluate the effect of Msi-1 expression upon IEC differentiation. Results of the RT-PCR analysis showed no change in expression of goblet cell-specific genes such as *MUC-2*, *TFF-3*, or *KLF-4* (Fig. 2B). Also, genes specific for absorptive cell lineage (Fig. 2B) or neuroendocrine cell lineage (data not shown) remained undetectable in both LS174T/GFP and LS174T/Msi-1 cells. In sharp contrast, expression of Paneth cell-specific genes such as *PLA2G2A*, *HD-5*, and *Lysozyme*[17] appeared to be decreased in LS174T/Msi-1 cells, compared with LS174T/GFP cells (Fig. 2B). This suggested that expression of Msi-1 might have suppressed expression of Paneth cell-specific genes in LS174T/Msi-1 cells.

To confirm our earlier results, we further examined the expression of one of the Paneth cell-specific genes, *PLA2G2A*, as it showed the clearest decrease in mRNA in LS174T/Msi-1 cells (Fig. 2B). Quantitative RT-PCR confirmed an up to 90% decrease of *PLA2G2A* mRNA expression in LS174T/Msi-1 cells, compared with LS174T/GFP cells (Fig. 3A). PLA2G2A protein secretion also showed a significant decrease in LS174T/Msi-1 cells compared with LS174T/GFP cells (Fig. 3B). From these results, Msi-1 appeared to suppress *PLA2G2A* gene expression at the mRNA level, leading to decreased secretion of mature PLA2G2A protein.

Expression of Msi-1 did not change the expression level of genes downstream of Notch and Wnt pathways in LS174T cells

As it is has been previously reported that one of the molecular functions of Msi-1 is translational repression of m-Numb, a negative regulator of Notch signaling,[10] we next examined whether suppression of *PLA2G2A* gene expression might be induced through modulation of the Notch signaling pathway. Immunoblot analysis of m-Numb or Hes1 expression, however, showed equivalent expression of both proteins in LS174T/Msi-1 and LS174T/GFP cells (Fig. 4A). Consistently, the reporter assay for RBP-Jk-dependent transcription showed no significant difference between LS174T/Msi-1 and LS174T/GFP cells (Fig. 4B). These results suggest that expression of Msi-1 had minimal effect upon expression of *m-Numb* or target genes of Notch in LS174T cells.

In addition to Notch, the Wnt signaling pathway has been described as another key signaling pathway for Paneth cell differentiation.[7,18] Also, *PLA2G2A* has been shown to be one of the direct target genes of the canonical Wnt pathway.[19] As a recent study reported that Msi-1 could modulate signaling of the Wnt pathway,[20] we next examined whether expression of Msi-1 had modulated the intracellular activity of the Wnt pathway. Consistent with the previous result in mammary

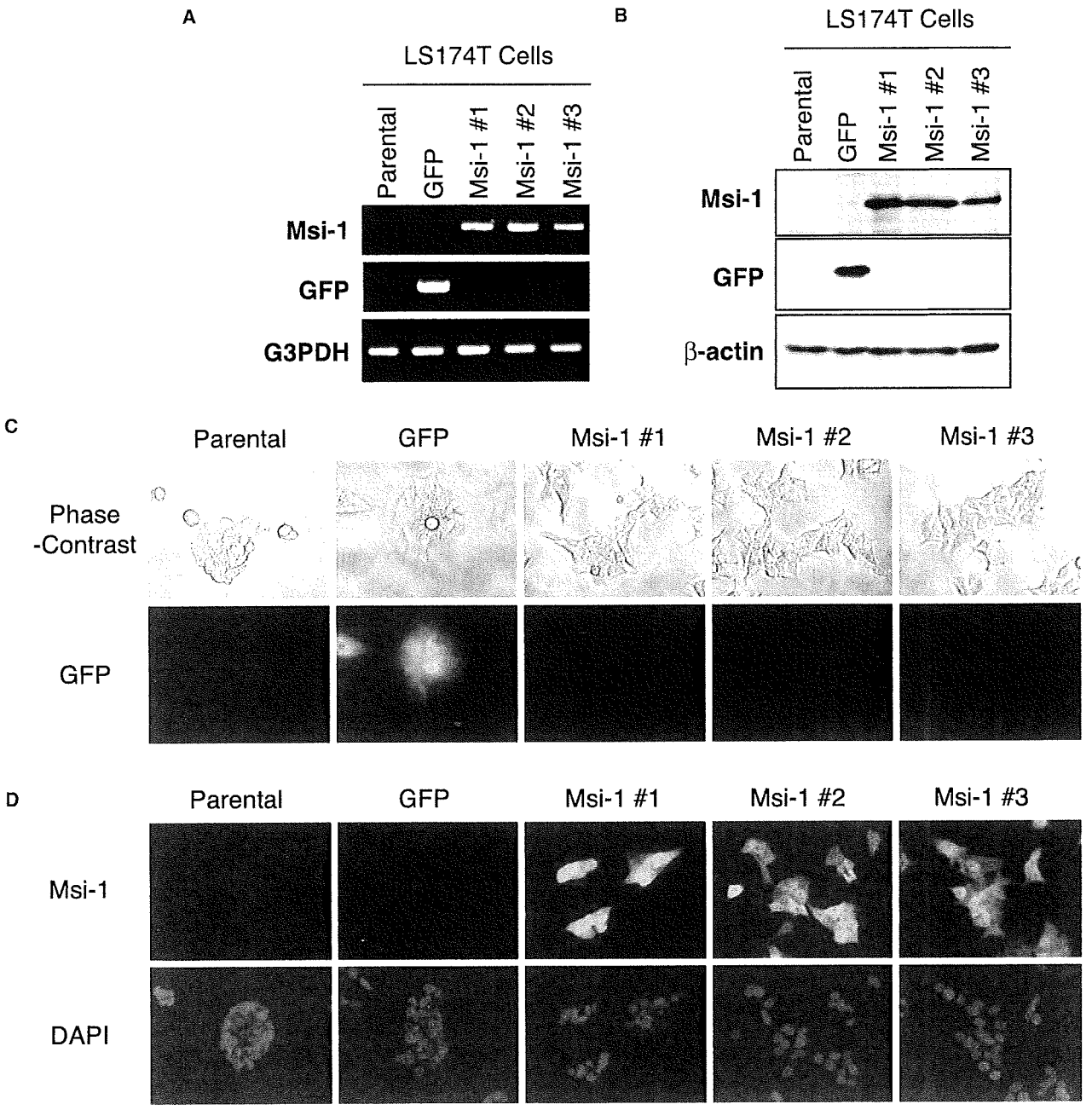

Fig. 1. Establishment of cell lines stably expressing Musashi-1. **A** Reverse transcriptase-polymerase chain reaction (RT-PCR) analysis of the generated cell lines. *GFP* (green fluorescent protein) indicates a clone of LS174T cells that constitutively expresses enhance green fluorescent protein (EGFP) (LS174T/GFP cells), whereas *Msi-1 #1*, *Msi-1 #2*, and *Msi-1 #3* indicate distinct clones of LS174T cell that constitutively express Musashi-1 (Msi-1) (LS174T/Msi-1 cells). *Parental* indicates the parental LS174T cells. Note that mRNA expression of Msi-1 or GFP is clearly observed in LS174T/GFP cells or LS174T/Msi-1 cells, respectively, but not in parental cells. **B** Immunoblot analysis of the generated cell lines. Total cell lysate obtained from each cell line was analyzed for expression of Msi-1, GFP, and β-actin. Msi-1 protein was detected exclusively in the LS174T/Msi-1 cell lines (Msi-1 #1, #2, and #3), whereas GFP protein was detected exclusively in LS174T/GFP cells (GFP). **C** Morphological changes and GFP expression in the generated cell lines. Phase contrast view of the cell lines shows aggregated, round colony formation in parental and LS174T/GFP cells (GFP), whereas a flat, monolayer expansion is observed in LS174T/Msi-1 cells (Msi-1 #1, #2, and #3). An epifluorescence view confirmed stable expression of GFP in LS174T/GFP cells, but not in other cells. **D** Expression of Msi-1 protein in generated cell lines. Cells were stained by Msi-1 specific antibody and visualized by Alexa-488-conjugated secondary antibody. Cells were also counterstained with 4′,6-diamino-2-phenylindole (DAPI). Staining confirmed the expression of Msi-1 protein in LS174T/Msi-1 cells (Msi-1 #1, #2, and #3), and not in other cells